Acta Crystallographica Section B
Structural Science
ISSN 0108-7681

Bis(μ^2-2-(dimethylamino)ethoxo-*N*,*O*,*O*)-di(phenolato-*O*)ditin(II): a high-resolution single-crystal X-ray diffraction and quantum chemical study

Alexander A. Korlyukov,[a] Victor N. Khrustalev,[a] Anna V. Vologzhanina,[a]* Konstantin A. Lyssenko,[a] Mikhail. S. Nechaev[b] and Mikhail Yu. Antipin[a]

[a]AN Nesmeyanov Institute of Organoelement Compounds, Russian Academy of Sciences, Vavilov str. 28, Moscow 119991, Russian Federation, and [b]Department of Chemistry, MV Lomonosov Moscow State University, Leninskie Gory 1/3, Moscow 119991, Russian Federation

Correspondence e-mail: vologzhanina@mail.ru

Received 8 February 2011
Accepted 12 June 2011

Experimental and calculated electron density functions $\rho(r)$ of the title compound in the crystal were obtained. These were compared with $\rho(r)$ for an isolated dimer. Application of the 'Atoms in Molecules' theory allowed the visualization of the electron lone pair (Lp) of tin(II) and the calculation of some bond energies and all atomic charges. The stereochemical activity of the Lp was demonstrated and its volume was estimated to be approximately 10 Å^3. The energies of N→Sn and Sn—O bonds were found to be 13–18 and 25–52 kJ mol^{-1}. According to the experimental, AM05-PW and PBE0/6-311G(d,p) calculation data, μ^2-2-(dimethylamino)ethoxoate accepts 0.68, 0.45 and 0.40 e from the Sn atom. Using the example of μ^2-2-(dimethylamino)ethoxoates and complexes of bis(*n*-butyl)tin(IV) it was demonstrated that the more screened the Sn atom, the better the catalytic activity of its complex in polyurethane synthesis.

1. Introduction

Divalent tin compounds are of continuing interest owing to their practical applications. Some tin(II) derivatives are used as catalysts in the synthesis of polyesters, polylactides (Dove *et al.*, 2006), organic polycarbonates (Davies, 2004) and polyurethanes (Chernov *et al.*, 2009). It is believed that their catalytic behaviour is related to the characteristics of a electron lone pair (Lp) on the Sn^{II} atom. In most donor-stabilized stannylenes R_2Sn, the Lp of the tin is stereochemicaly active, and its position depends on the type of Sn^{II} coordination polyhedron.

Stannylenes with simple alkyl and aryl groups are reactive compounds and readily undergo oligomerization and insertion in C—H, C—*X* and multiple bonds (Neumann, 1991; Egorov & Gaspar, 1995; Barrau & Rima, 1998). Besides, tin compounds are biologically active (Orita *et al.*, 1999; Hori & Hagiwara, 1999) or even toxic (*DOSE*; Royal Society of Chemistry, 1999; Lewis, 2000). Thus, the search for non-toxic and stable catalysts becomes an important task. Non-toxic tin derivatives include compounds that do not contain tin–carbon bonds. The stabilization of a tin(II)-containing compound can be achieved by the introduction of bulky groups which also screen a Lp. Thermodynamic stabilization due to the electronic effects of a ligand is also possible. At the same time, using the example of polylactide synthesis Dove *et al.* (2006) proposed that polymerization reactions activated by the divalent tin should be more reasonably described as a *lone-pair-dominated* process rather than a *ligand-assisted* process. Thus, the characteristics of a Lp in a tin-containing catalyst are of interest. Previous quantum chemical calculations have shown that these Lps generally have an *s*-character; at the same time Sn can participate in a strong coordination inter-

Table 1
Experimental details for (I).

Crystal data	
Chemical formula	$C_{20}H_{30}N_2O_4Sn_2$
M_r	599.84
Crystal system, space group	Orthorhombic, *Pbca*
Temperature (K)	100
a, *b*, *c* (Å)	13.0745 (2), 12.9669 (2), 13.6824 (3)
V (Å^3)	2319.66 (7)
Z	4
Radiation type	Mo *Kα*
μ (mm^{-1})	2.18
Crystal size (mm)	0.19 × 0.12 × 0.07
Data collection	
Diffractometer	Bruker Apex II CCD area detector
Absorption correction	Multi-scan† *SADABS* (Sheldrick, 1998)
T_{min}, T_{max}	0.796, 0.914
No. of measured, independent and observed [$I > 2\sigma(I)$] reflections	203 973, 12 165, 7690
R_{int}	0.037
Refinement	
$R[F^2 > 2\sigma(F^2)]$, $wR(F^2)$, *S*	0.023, 0.092, 1.00
No. of reflections	12 165
No. of parameters	187
No. of restraints	0
H-atom treatment	All H atom parameters refined
$\Delta\rho_{max}$, $\Delta\rho_{min}$ (e Å^{-3})	1.45, −1.17

Computer programs used: *APEX*2 (Bruker, 2005), *SHELXTL* (Sheldrick, 2008), *SADABS* (Sheldrick, 1998). † Based on symmetry-related measurements.

action with electron lone pairs of donor atoms (O and N) using its unoccupied *p*-orbitals (Nechaev & Ustynyuk, 2005).

Among a huge number of tin(II) compounds, we concentrated our attention on the 2-(dimethylamino)ethoxoates of the $Sn(OCH_2CH_2NMe_2)X$ type (see scheme below). The compounds do not contain bulky groups; nevertheless, they are stabilized due to the presence of acceptor substituents (oxygen and *X*) and a coordination bond (with nitrogen). The key features of the compounds are:

(i) the electron lone pair, as well as

(ii) the partially occupied p_z-orbital of an Sn atom, and

(iii) labile strongly polarized Sn—O and Sn—*X* bonds.

Chernov *et al.* (2009) proved the catalytic activity of $Sn(OCH_2CH_2NMe_2)(OR)$ (*R* = Me, Et, ^{i}Pr, ^{t}Bu, Ph) in polyurethane synthesis. The goal of the present paper is to discover the characteristics of the Lp of the Sn^{II} atom and to evaluate the strength of the Sn—O and Sn—N bonds as well as the role of crystal packing in the geometry of $Sn(OCH_2CH_2NMe_2)X$.

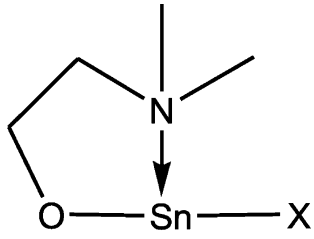

Detailed analysis of electron structure is possible in the framework of Bader's (1990) 'Atoms in Molecules' theory (AIM). According to the AIM theory, information on chemical bonding can be obtained by analyzing local minima, maxima and saddle points of an electron density $\rho(r)$ function. The characteristics of $\rho(r)$ at critical points that correspond to chemical bonds [CP(3,−1)] are the most important for the qualitative and quantitative description of the electronic structure. Another advantage is the possibility of evaluating the energies of closed-shell interactions as well as interactions of the intermediate type using the correlation proposed by Espinosa *et al.* (1998)

$$E_{A-B} \simeq -\frac{1}{2}V^e(r), \qquad (1)$$

where E_{A-B} is the energy of a weak interatomic contact or a coordination bond and $V^e(r)$ is the potential energy density in the corresponding CP(3,−1). The value of $V^e(r)$ can be calculated from values of $\rho(r)$ and $\nabla^2\rho(r)$ at CP(3,−1) using the Kirzhnitz formula for kinetic energy density and local virial theorem expression (Kirzhnitz, 1957; Abramov, 1997). The correlation shown in (1) was initially proposed for hydrogen bonds; however, it gives sufficiently accurate estimates for almost any bond characterized by a positive value of $\nabla^2\rho(r)$, *e.g.* in the case of the *M*—*X* bond, where *M* = main group or transition metal and *X* = N, O, C or halogen (Borissova *et al.*, 2008; Tikhonova *et al.*, 2009).

2. Experimental

2.1. Investigation objectives

The electron-density distribution function $\rho(r)$ was investigated for $Sn(OCH_2CH_2NMe_2)(OPh)$ (I) both in the isolated molecule and in the solid state. The synthesis of the title compound has been described by Chernov *et al.* (2009). A crystal suitable for X-ray diffraction analysis was crystallized from THF (tetrahydrofuran) solution. The screening of an Sn atom was investigated within the framework of the stereoatomic model (Blatov & Serezhkin, 2000). Eleven 2-(dimethylamino)ethoxoates (*L*) and eight bis(*n*-butyl)tin(VI)-containing complexes found from the Cambridge Structural Database, release 2010 (Allen, 2002), were taken into consideration.

2.2. Crystal structure determination

X-ray diffraction experiments of (I) were carried out on a Bruker APEX II CCD at 100 K. The absorption correction was carried out using *SADABS* (Sheldrick, 1998). The structure was solved by direct methods and refined by the full-matrix least-squares technique against F^2 in an anisotropic (for non-H atoms) approximation. All H atoms were located in difference-Fourier maps and refined in an isotropic approximation. The calculations were performed using *SHELXTL*, Version 5.0 software (Sheldrick, 2008). Crystallographic parameters and details of the refinement are given in Table 1.

2.3. Electron-density distribution

An experimental electron-density distribution was obtained by means of a multipole refinement. It was carried out within the Hansen–Coppens formalism (Hansen & Coppens, 1978) using the *XD* program package (Koritsansky *et al.*, 2003) with the core and valence electron density derived from wavefunctions fitted to a relativistic Dirac–Fock solution (Su & Coppens, 1998). All C—H distances were normalized to 1.08 Å before the refinement. The level of multipole expansion was hexadecapole for an Sn atom, octapole for other non-H atoms and dipole for H atoms. The refinement was carried out against F and converged to $R = 0.0162$, $wR = 0.0190$ and GOF = 1.58 for 7690 merged reflections with $I > 3\sigma(I)$. All bonded pairs of atoms satisfied the Hirshfeld criteria. The residual electron-density peaks did not exceed 0.37 e Å^{-3}.

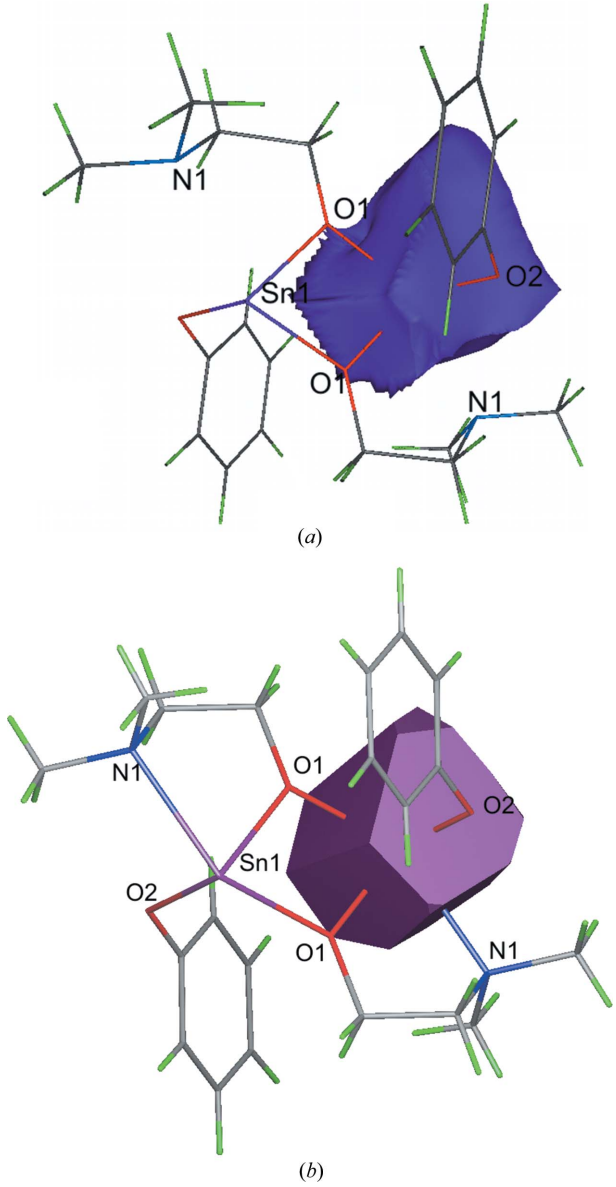

Figure 1
Zero-flux surface of the Sn atom in (I) obtained within AIM (*a*) and stereoatomic (*b*) approaches.

Topological analysis of the $\rho(r)$ function was carried out using the *WinXPRO* program package (Stash & Tsirelson, 2002).

The role of crystal packing was estimated using quantum-chemical calculations: the quantum chemical calculations of (I) in the crystal were carried out using the *VASP*5.2.8 code (Kresse & Furthmüller, 1996*a*,*b*; Kresse & Hafner, 1993). The conjugate gradient technique was used for optimizations of the atomic positions (starting from the experimental data) and minimization of the total energy. The projected augmented wave (PAW) method was applied to account for core electrons, while valence electrons were approximated by plane-wave expansions with 400 eV cut-offs. Exchange and correlation terms of the total energy were described by the AM05 exchange-correlation functional, which is more accurate for the description of dipole–dipole interactions than conventional pure functionals (Armiento & Mattsson, 2005; Mattsson & Mattsson, 2009). In the final step of our calculations the maximum residual forces on atoms were less than 0.02 eV Å^{-1}, and energy variations were less than 10^{-3} eV. To carry out the topological analysis of the electron-density distribution function in terms of the AIM theory, a dense FFT (fast-Fourier transformation) grid of 432 × 432 × 480 points was used. The latter was obtained by a separate single-point calculation of the optimized geometry with small-core PAWs for each atom type. The topological analysis of the electron-density distribution function was carried out using the AIM program – part of the *ABINIT* software package (Gonze *et al.*, 2002).

Density functional theory: An isolated molecule of (I) was studied on the PBE0/6-311G(d,p) level of theory (a double-zeta valence potential all-electron basis set was applied to the Sn atom because of the absence of an appropriate all-electron basis set of triple-zeta quality). Vibrational frequencies were calculated to check the stability of the atomic configuration obtained in the optimization procedure. All calculations were carried out using the *GAUSSIAN*03W program (Frisch *et al.*, 2004). The topological analysis of the calculated electron density for the isolated molecule (I) was carried out *via* the *AIMALL* program (Keith, 2009).

2.4. Stereoatomic model of crystal structures

To evaluate the characteristics of a Lp in tin-containing compounds, the $\rho(r)$ functions should be obtained for a number of systems. Unfortunately, it is just not possible to cover the whole set of these compounds by topological analysis. However, this problem can be overcome by the application of the stereoatomic model. Within this model of a crystal structure (Blatov & Serezhkin, 2000), an atom is represented as the corresponding Voronoi–Dirichlet polyhedron (VDP). The VDP of an A atom surrounded by $\{Y_i\}$ atoms is a convex polyhedron formed by planes that are drawn perpendicular to A–Y_i contacts at their midpoints (see also the supplementary information[1]). Indeed, the similarity of a tin

[1] Supplementary data for this paper are available from the IUCr electronic archives (Reference: GW5015). Services for accessing these data are described at the back of the journal.

Table 2
Experimental and calculated structural parameters for (I) (Å, °).

Parameter†	Experiment	AM05-PW	PBE0/6-311G(d,p)
N1→Sn1	2.4718 (14)	2.486	2.503
Sn1—O1	2.1179 (11)	2.139	2.165
Sn1—O1^{i}	2.2453 (11)	2.251	2.241
Sn1—O2	2.0893 (13)	2.117	2.111
Sn1—Sn1^{i}	3.5920 (2)	3.615	3.627
N1—Sn1—O1	73.13 (5)	73.1	72.0
N1—Sn1—O2	81.58 (5)	81.8	79.1
O1—Sn1—O2	93.01 (5)	92.9	91.3
O1—Sn1—O1^{i}	69.21 (5)	69.2	69.2
Δ(Sn)	0.92	0.84	1.14

† Symmetry code: (i) $-x, y+2, -z$. Δ(Sn) is the value of the shift of the Sn atom from the centre of its coordination polyhedron.

atomic domain and VDP in (I) is visually demonstrated in Fig. 1. Some characteristics of the tin VDP in (I) are listed in Table 1S. Among all VDP characteristics, its volume (V_{VDP}) and the solid angle of the VDP faces (Ω_{ij}, expressed as a percentage of 4π steradians) are of interest to us. The former estimates the volume of the atomic domain, and the latter is roughly proportional to the strength of an $A-Y_i$ interaction. The VDP of all atoms and Ω values for intermolecular interactions were calculated by means of the program package *TOPOS* (Blatov, 2006).

Recently Blatov (2004) proposed an analogy between some descriptors of the VDP and properties of the $\rho(r)$ function. The central point of a VDP corresponds to a global maximum (critical point [3,−3)], the VD polyhedra vertices to (3,+3) critical points, and faces and edges to saddle points (3,−1) and (3,+1), respectively. Thus, we tested this assumption on the example of (I). More than 20 tin contacts were found within the framework of the stereoatomic model, nevertheless, 12 of them are indirect and cannot be interpreted as bonding interactions (Table 1S). Among direct contacts all the bonds were found which were revealed from the $\rho(r)$ analysis. Six of seven tin bonds are characterized by $\Omega > 5\%$. Besides, ring and cage critical points are situated near VDP vertices or edges (average deviation is equal to 0.7 Å). Thus, the results of these independent methods are in satisfactory agreement with each other.

3. Results and discussion

3.1. Molecular geometry

The molecular structure of (I) is given in Fig. 2. Some structural parameters of (I) in the crystal and those for the isolated dimer are listed in Table 2. The Sn atom in (I) adopts distorted trigonal bipyramidal geometry with N1 and O1^{i} atoms occupying the axial positions, O1, O2 and a Lp in the equatorial positions [symmetry code: (i) $-x, 2-y, -z$]. The stereochemically active lone pair of the Sn atom pushes the atoms at the axial positions towards the equatorial bonded atoms.

All bonds involving the Sn atom obtained from the AM05-PW calculation are elongated in comparison with the experimental ones. The elongation is most pronounced for the Sn1—O2 bond. As for the isolated dimer, the Sn1—O1^{i} bond length was obtained as being shorter than that in the crystal structure, whilst the increase in the N1→Sn1, Sn1—O1 bond lengths and the shift of the Sn atom from the centre of its coordination polyhedron are more pronounced than those in the AM05-PW calculation. Both AM05-PW and PBE0 calculations give the difference between the experimental and calculated bond distances as less than 0.05 Å. The geometry obtained in AM05-PW calculations is closer to the experimental data than that produced by the PBE0 calculation due to the higher level of theory. In general, the quantum chemical calculations reproduced satisfactorily the experimental structural parameters.

3.2. Peculiarities of the chemical bonding in (I)

Topological analysis of the experimental and calculated $\rho(r)$ in the crystal of (I) has revealed the presence of critical points CP(3,–1) in the regions of all the expected chemical bonds (Table 2S). In the Lp area additional CPs (3,–1) were found which corresponded to intra- (with the C10 atom) and intermolecular contacts (with H8 and H3*B* atoms). It is worth mentioning that the intramolecular contact Sn1—C10 is also observed in the isolated dimer. In contrast with silicon- and germanium-containing complexes with a coordination number of 5 (Vologzhanina *et al.*, 2008), more than one intermolecular interaction with $\Omega > 5\%$ and $T\cdots A-D > 110°$ (A = Si, Ge, Sn; D = nucleophile) is observed in the crystal of (I). Indeed,

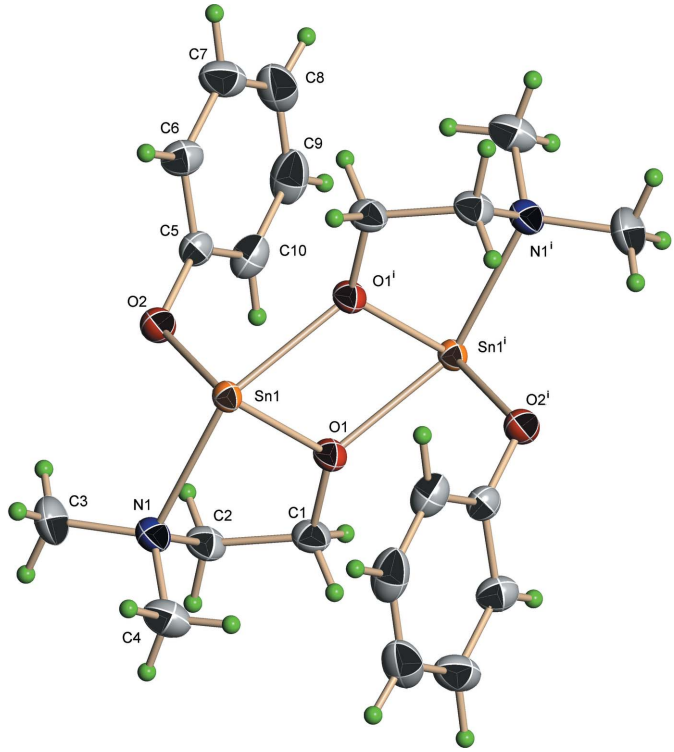

Figure 2
Molecular view of (I) with displacement ellipsoids at a probability level of 70%. Symmetry code: (i) $-x, 2-y, -z$.

Table 3
Bonding energies (kJ mol^{-1}) of the bonds involving the Sn atom in (I).

Bond	Experiment	AM05-PW	PBE0/6-311G(d,p)
N1→Sn1	52.54	76.79	55.73
Sn1—O1	144.49	204.82	123.97
Sn1—O1^{i}	105.09	134.90	99.52
Sn1—O2	183.93	218.13	143.61
Sn1—C10^{i}	3.60	3.18	1.93
Sn1—H8^{ii}	2.64	3.31	–
Sn1—H3*B*^{iii}	2.01	–	–

Symmetry codes: (i) $-x, 2-y, -z$; (ii) $-x+\frac{1}{2}, y-\frac{1}{2}, z$; (iii) $x, -y+\frac{3}{2}, z+\frac{1}{2}$.

H8$^{ii}\cdots$Sn1—O1^{i} and H3*B*$^{iii}\cdots$Sn1—N1 contacts [symmetry codes: (i) $-x, 2-y, -z$; (ii) $-x+\frac{1}{2}, y-\frac{1}{2}, z$; (iii) $x, -y+\frac{3}{2}, z+\frac{1}{2}$] are characterized by Ω = 9.2 and 6.7%, and H$\cdots$Sn—*D* = 175 and 131°.

The values of the calculated topological parameters (Table 2S and Table 3) are in semi-quantitative agreement with the experimental data. In general, the absolute values of PW-DFT topological characteristics exceed those obtained from the multipole refinement of the experimental $\rho(r)$ value. A comparison of the topological parameters calculated for the isolated dimer with those obtained from experiment and AM05-PW calculations revealed noticeable changes in the Sn1—O2 bond. It can be assumed that such differences between the crystalline state and the isolated dimer are caused by crystal packing forces. Indeed, the O1 and N1 atoms only take part in the intramolecular chemical bonding with the Sn atom and in the formation of the complex. At the same time the O2 atom, in accordance with the experimental $\rho(r)$, is involved not only in chemical bonding with Sn, N and C atoms, but also in three O$\cdots$H contacts (see also the supplementary information). The presence of intermolecular bonds may explain the discrepancies between either geometry and $\rho(r)$ parameters of the Sn1—O2 bond in the crystal and in the gas phase.

It is noteworthy that the PW-DFT energies calculated using correlation (1) systematically exceed the experimental ones (Table 3). Besides, both the experimental and PW-DFT topological parameters surpass (with the exception of E_{bond} for Sn1—N1) those calculated at the PBE0/6-311G(d,p) level of theory. Taking into account that some bond distances in the isolated dimer are closer to the experimental values than for geometry obtained with PW-DFT calculations, these discrepancies can be explained by the overestimation of $V^{e}(r)$ values calculated by the Kirzhnitz formula (Kirzhnitz, 1957) and the shortcomings of the correlation proposed by Espinosa *et al.* (1998).

Unfortunately, it is difficult to verify the correctness of the estimated bond energies because data on the estimation of valence Sn—O and coordination Sn—N bond energies are limited. In accordance with Nechaev & Ustynyuk (2005), the energy of the $Me_2N\rightarrow Sn$ bond in $[(Me_3Si)_2NSnL]_2$ is 36.0 kJ mol^{-1}. At the same time, Strenalyuk *et al.* (2008) estimated the E_{bond} for Sn—N to be 61.71 kJ mol^{-1} in the structure of phthalocyaninatotin(II) [*r*(Sn—N) = 2.042 Å]. The latter value is closer to E_{bond}(N→Sn) obtained from $\rho(r)$ in (I). As for Sn—O bonds, Wakamatsu *et al.* (2008) found the ΔH value of hydroxydistannoxane dimerization (MP2/6-311+G(d)) to be 208.08 kJ mol^{-1}. The latter process led to the formation of two Sn—O coordination bonds (2.17 and 2.09 Å). On the other hand, PW-DFT calculated energies of a thf→Sn bond in a number of $(CO)_5MSnCl_2\cdot n$THF complexes (*M* = Cr, W; *n* = 1, 2) vary from 41.87 to 75.78 kJ mol^{-1} (Aysin *et al.*, 2010), whilst *r*(O→Sn) change from 2.081 to 2.401 Å. The Sn—O bond energies in (I) are higher than for the above-mentioned results because we obtained results for the formally covalent bonds. Indeed, in the structure of Ph_3SnOH E_{bond}(Sn—O) = 379.32 kJ mol^{-1} (Luo, 2007), experimental Sn—O bond lengths are 1.962 Å (Lo *et al.*, 1999). This indicates that the obtained bond energies are rather reasonable.

3.3. Lone-pair characteristics

The diffuse character of localized lone pairs of heavy atoms in comparison with those of lighter elements was demonstrated in a number of papers. For example, Malcolm *et al.*

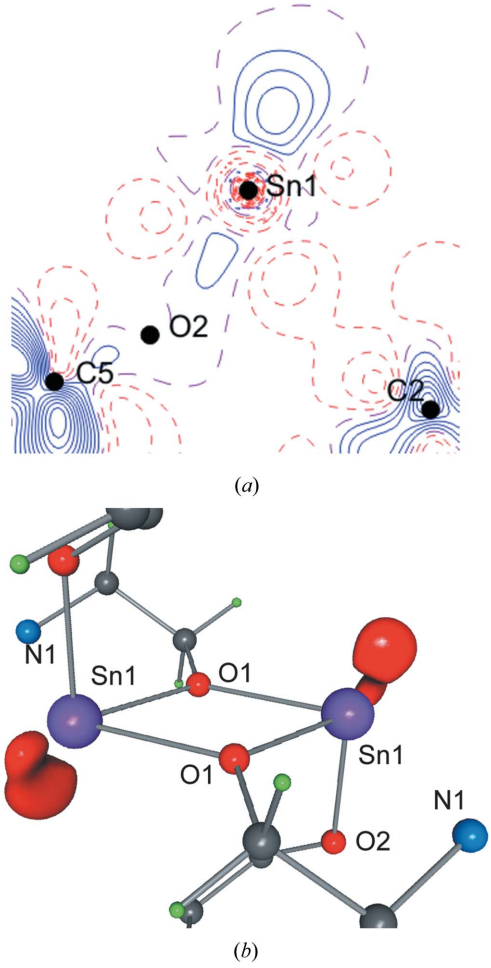

Figure 3
Lp represented with deformation electron density maps in the tin section including the Sn1, C5, C2 atoms [(*a*) the regions of $\rho(r)$ concentration are shown by solid lines; isolines are drawn through 0.1 e Å^{-3}, negative contours are dashed] and as a three-dimensional view [(*b*) shell +0.1 e is given].

Table 4
Selected experimental and calculated AIM atomic charges (e) in (I).

Atom	Experiment	AM05-PW	PBE0/6-311G(d,p)
Sn1	1.50	1.30	1.37
O1	−0.95	−1.09	−1.24
O2	−0.92	−1.14	−1.25
N1	−0.82	−1.02	−1.08

Table 5
Selected experimental and calculated atomic volumes in (I) (Å^3).

Atom	Experiment	V_{VDP}	AM05-PW	PBE0/6-311G(d,p)
Sn1	30.03	17.58	30.20	38.07
O1	12.17	11.50	12.12	13.25
O2	15.22	11.88	15.38	17.34
N1	8.45	6.54	8.82	8.99

(2002) have localized Lps of metal atoms (*E*) in the molecules H*EE*H, Me*EE*Me, Me$_2$*EE*Me$_2$ and H$_2$*EE*H$_2$ (*E* = Si, Ge, Sn) and have shown that the heavier the element, the more diffuse its Lp. Abrahams *et al.* (2006) proved the larger stereochemical activity of the tin Lp in comparison to lead analogues both in the gas phase and in crystals of Sr(MX_3)$_2$·5H$_2$O type (*M* = Sn, *X* = Cl, Br; *M* = Pb, *X* = Br). Stoltzfus *et al.* (2007) came to the same conclusion for Sn *versus* Pb and Bi under the investigation of *E*WO$_4$. Besides, Stoltzfus *et al.* (2007) mentioned the almost spherical character of the Lps of heavy elements whenever they are present in a structure.

Deformation electron density (DED), which is the difference between an experimental electron density and a superposition of electron densities of independent atoms placed at experimental positions, in the region of the Sn atom was analyzed. A graphical map is given in Fig. 3. It was found that the Lp of Sn deviates from the O1—Sn1—N1 and O1—Sn1—O2 planes. Thus, the DED map indicates the increased asphericity of the electron density in the region of the Sn atom rather than the real position of a Lp. Thus, a more reliable analysis of the position of the Lp was carried out using the electron localization function (ELF) calculated from the experimental data (Tsirelson & Stash, 2002; Figs. 3 and 4). Topological analysis of the theoretical ELF enables the location of the real space regions in which pairs of electrons are most likely to be found (Silvi & Savin, 1994). ELF contour maps in the planes of tin bonds in (I) revealed the presence of a concentration of valence electron density near the Sn atom which cannot be assigned to any Sn bond (Fig. 2S). As seen from the figures, the results obtained coincide with most of our assumptions about the type, shape and volume of a tin Lp. In particular, the Lp can be located both in experimental and calculated crystal structures and in the gas phase. It is directed towards an 'empty' region which is not occupied by Sn—O or Sn—N bonds. The shape of the valence electron density domain in crystals differs from that of the isolated molecule (Fig. 4). In the latter case the shape of a Lp can be described as an almost undistorted hemisphere. Crystal packing effects led to a decrease in volume and change in the shape of the tin Lp (Fig. 4). The tin Lp in the crystal can be described as the half of torus that is doubly concave in the direction perpendicular to the Sn–Lp vector. The authors of the above-mentioned reports devoted to the investigation of tin Lp do not mention a distortion or an asphericity of the lone pair. Thus, a flattened Lp in the structure of organotin compounds was not observed before.

3.4. Atomic charges and volumes

Atomic charges were calculated by integration of $\rho(r)$ over the atomic basins surrounded by zero-flux surfaces. The experimental and AM05-PW calculated values are in a satisfactory agreement. We obtained a positive charge for the Sn atom and negative charges for O and N atoms (Tables 4 and 2S). Tin charge values obtained from AM05-PW, PBE0/6-311G(d,p) and experiment are equal to 1.30, 1.37 and 1.50 e. As expected, the OPh group is more negatively charged than in 2-(dimethylamino)ethoxoate. The overall charge of 2-(dimethylamino)ethoxoate obtained from experiment, AM05-PW and PBE0/6-311G(d,p) calculations is equal to −0.32, −0.54 and −0.60 e. Taking into account its formal charge (−1 e), the amount of charge density transferred from the Sn atom to this group can be calculated. In accordance with this procedure 2-(dimethylamino)ethoxoate being a bridge-chelate ligand accepts 0.68, 0.46 or 0.40 e from the tin.

Atomic volumes were calculated using an analogous procedure. The sum of the atomic volumes in the crystal (288.78 and 292.60 Å^3 for experimental and AM05-PW data) reproduces well the unit-cell volume per (I) moiety (289.96 Å^3). As expected, the volume of the isolated dimer

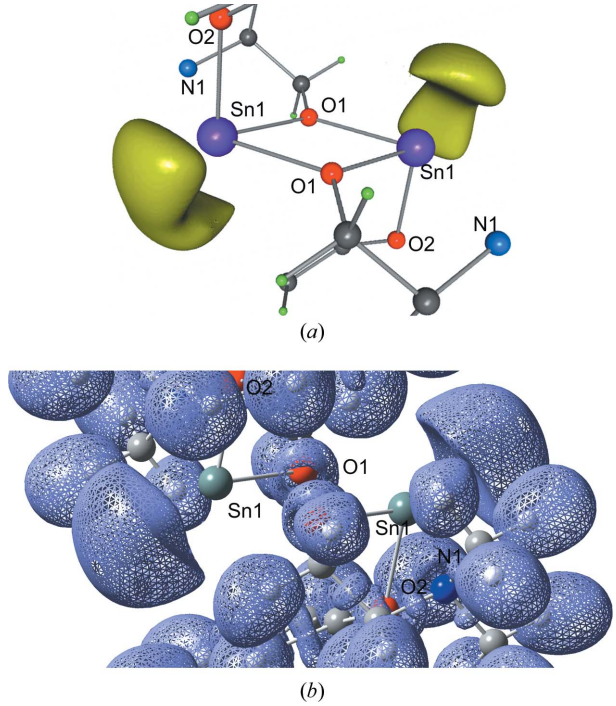

Figure 4
Lp represented with ELF distribution (*a*) in the crystal and (*b*) in the isolated dimer given with the η = 0.85 isosurface.

Table 6
Some VDP parameters of tin complexes with 2-(dimethylamino)-ethoxoate and *n*-butyl moieties.

CP(Sn): composition of tin coordination polyhedron including electron lone pair (Lp); V_{VDP}(Sn): the volume of tin Voronoi–Dirichlet polyhedron; $\Omega_{Rank\,=\,0}$(Sn): the sum of body angles corresponding to the tin faces with Rank = 0.

N	Compound	CP(Sn)	V_{VDP}(Sn) (Å^3)	$\Omega_{Rank\,=\,0}$(Sn) (%)	Refcode	Reference
(I)	$[Sn^{II}L(PhO)]_2$	NO_3Lp	17.58	18.93		Chernov *et al.* (2009)
(II)	$[Sn^{II}L(^tBuO)]_2$	NO_3Lp	18.50	17.68		Chernov *et al.* (2009)
(III)	$[Sn^{II}L_2Cd(acac)]_2$·thf	NO_3Lp	16.60	7.86	JERTEG	Hollingsworth *et al.* (2006)
(IV)	$[Sn^{II}LCl]_2$	NO_3Lp	19.13	23.65	PITGOP	Khrustalev, Portnyagin *et al.* (2007)
(V)	$[Sn^{II}LF]_2$	NO_3Lp	17.26 17.23	26.32 26.57	PITGUV	Khrustalev, Portnyagin *et al.* (2007)
(VI)	$[Sn^{II}L(N(SiMe_3)_2)]_2$	N_2O_2Lp	16.29 16.14	5.86 5.43	GARXIH	Khrustalev, Portnyagin *et al.* (2007)
(VII)	$Sn^{II}L_2$	N_2O_2Lp	19.94	20.72	GUZRIC	Zemlyansky *et al.* (2003)
(VIII)	$[Sn^{II}LN_3]_2$	N_2O_2Lp	18.53	23.46	KAJVEX	Khrustalev, Portnyagin, Zemlyansky, Borisova, Ustynyuk *et al.* (2005)
(IX)	$Li_2[Sn^{II}L_3Fe(CO)_4]_2$	NO_3Fe	13.02	0	NIYNAF	Khrustalev *et al.* (2008)
(X)	$[Sn^{II}L_2Fe(CO)_4]$	N_2O_2Fe	12.97 13.67	0.04 0.22	YIKQUF YIKQUF01	Khrustalev, Zemlyansky *et al.* (2007)
(XI)	$[Sn^{IV}L_2PhCl]$	N_2O_2CCl	11.05	0	WEQRIU	Portnyagin *et al.* (2006)
(XII)	$[Sn^{IV}(^nBu)_2((C_5H_4COO)Co(C_4(C_6H_5)_4))_2]$·$CHCl_3$	C_2O_4	11.66	0	LERLOK	Kumar *et al.* (2006)
(XIII)	$[Sn^{IV}(^nBu)_2(C_5H_3S_3CH_2COO)_2]$	C_2O_4	11.72	4.67	QEQLEE	Lu *et al.* (2006)
(XIV)	$[Sn^{IV}(^nBu)_2(C_6H_3(NO_2)_2COO)_2]$·$C_6H_5CH_3$	C_2O_4	12.06	0.84	SEZMUG	Win *et al.* (2007*a*)
(XV)	$[Sn^{IV}(^nBu)_2(C_6H_4(NMe_2)COO)_2]$	C_2O_4	11.62	0.74	SEZZED	Win *et al.* (2007*b*)
(XVI)	$[Sn^{IV}(^nBu)_2(C_6H_4(NC_5H_8ON)COO)_2]$	C_2O_4	11.51	0	SIVGEK	Baul *et al.* (2008)
(XVII)	$[Sn^{IV}(^nBu)_2(C_6H_4(NO_2)COO)_2]$	C_2O_4	11.69	0.38	TAPGEW	Harston *et al.* (1992)
(XVIII)	$[Sn^{IV}(^nBu)_2((C_{30}H_{31}Ge)COO)_2]$	C_2O_4	12.04	1.66	ULIKUN	Imtiaz-ud-Din *et al.* (2003)
(XIX)	$[Sn^{IV}(^nBu)_2((C_{12}H_8N_2OBr)COO)_2]$	C_2O_4	11.87	0	XAKQQQ	Baul *et al.* (2004)

was found to be larger (335.13 Å^3) than in the crystal. It is worth mentioning that atomic volumes in the gas phase are usually 1–2 Å^3 larger than those in the crystal. The only exception is the Sn atom, which is characterized by experimental, AM05-PW and PBE0/6-311G(d,p) volumes equal to 30.03, 30.20 and 38.07 Å^3. In our opinion, this fact comes from the more diffuse character of the Lp of tin in the gas phase.

3.5. Analyses of tin 2-(dimethylamino)-ethoxoates within the stereoatomic model

Atomic volumes calculated within the stereoatomic and AIM models differ significantly (Tables 5 and 3S). Thus, only a relative volume of a tin(II) lone pair can be estimated. The structures of 11 compounds containing tin and 2-(dimethylamino)ethoxoate have been investigated to date (Table 6). Most of them are tin(II) compounds with the exception of $[Sn^{IV}L_2PhCl]$ (WEQRIU; Portnyagin *et al.*, 2006). The latter is also a unique compound with the coordination number (CN) equal to 6. The others are characterized by CN(Sn) = 4 and a trigonal bipyramidal geometry of a tin polyhedron with a lone pair [(I)–(VIII)] or Fe atom [(IX) and (X)] in one equatorial position. 2-(Dimethylamino)ethoxoate reacts as a bridge-chelate [(I)–(VI), (VIII)], chelate [(VII), (IX)–(XI)] or bridge [(III) and (IX)] ligand. Nevertheless, $V_{VDP}(Sn^{II})$ remains constant [$\simeq$ 18 (1) Å^3] for all complexes with a Lp and is 5–7 Å^3 larger than that for iron- or tin(IV)-containing complexes. Although this value is almost two times smaller than the atomic domain volume calculated within the AIM approach, it allows the volume of the Lps to be estimated as being approximately 1/3 of the volume of tin. Taking into account the experimental and AM05-PW volume (30 Å^3) of the Sn atom obtained within AIM theory, one can estimate the volume of its Lp as approximately 10 Å^3.

Although the volume of the Lp of tin(II) in 2-(dimethylamino)ethoxoates seems to be constant, the complexes display variable catalytic activity in polyurethane formation. Chernov *et al.* (2009) compared the activity of (I), (II), (VI), (VII) and dibutyltin dilaurate (DBTDL, industry standard catalyst) in the reaction between polyethylene glycol and hexamethylene diisocyanate. The 'gel time' under an argon atmosphere and catalyst concentrations of > 0.2 mol% increased as

$$\text{DBTDL} < (\text{VI}) \simeq (\text{II}) < (\text{I}) < (\text{VII}). \qquad (2)$$

The catalytic activity is expected to depend on the stereochemical activity of the Lp. We suggest that this property is proportional to the area of the tin's coordination sphere which is only involved in the intermolecular interactions; *e.g.* it can be calculated as the sum of solid angles of tin VDP faces with Rank = 0 [$\Omega_{Rank\,=\,0}$(Sn)]. The different 'activity' of the tin lone pairs is visually demonstrated in Fig. 5. Unfortunately, the crystal structure of DBTDL was not obtained beforehand; thus, in order to estimate $\Omega_{Rank\,=\,0}$(Sn) for this complex the structures of ordered mononuclear discrete bis(*n*-butyl)-tin(IV) complexes (XII)–(XIX) with carboxylic acids were taken from the CSD.

In accordance with the data obtained (Table 6), the value of the tin body angles for VDP faces with Rank = 0 in the structure of bis(*n*-butyl)tin(IV) depends on the disposition of butyl fragments and varies from 0 to 4.67%. Thus, the value of $\Omega_{\mathrm{Rank}=0}$(Sn) in the structure of DBTDL is expected to be less than 5%. The value of $\Omega_{\mathrm{Rank}=0}$(Sn) in the structures of DBTDL, (VI), (II), (I) and (VII) is equal to

$$\sim 1, 6, 18, 19 \text{ and } 21\%. \quad (3)$$

Thus, tin(II) 2-(dimethylamino)ethoxoates showed the anticipated trends in $\Omega_{\mathrm{Rank}=0}$(Sn) value [trend (3)] and the catalytic activity in polyurethane formation [trend (2)]. The remaining tin 2-(dimethylamino)ethoxoates with unshared Lp, except $[Sn^{II}L_2Cd(acac)]_2$, are characterized by $\Omega_{\mathrm{Rank}=0}$(Sn) > 20% and are expected to have large 'gel time'.

4. Conclusions

The topological analysis of a tin(II)-containing complex has been carried out. The energies of N→Sn and Sn–O bonds were found to be 52.5–76.8 and 99.5–218.1 kJ mol^{-1}. Experimental and theoretical energies were stated to be in qualitative agreement. 2-(Dimethylamino)ethoxoate was found to be an acceptor ($\simeq 0.7$ e) of charge with respect to tin(II). The presence of a tin electron lone pair causes the additional closed-shell interactions of tin to appear. The visualization of a lone pair confirmed its stereochemical activity, with the degree of distortion less significant in the gas phase. The use of the stereoatomic model allowed the quantitative estimation of the stereochemical activity in a lone pair. It was proposed that the less active the lone pair in the complex, the higher the catalytic activity in the polyurethane formation exhibited by the complex.

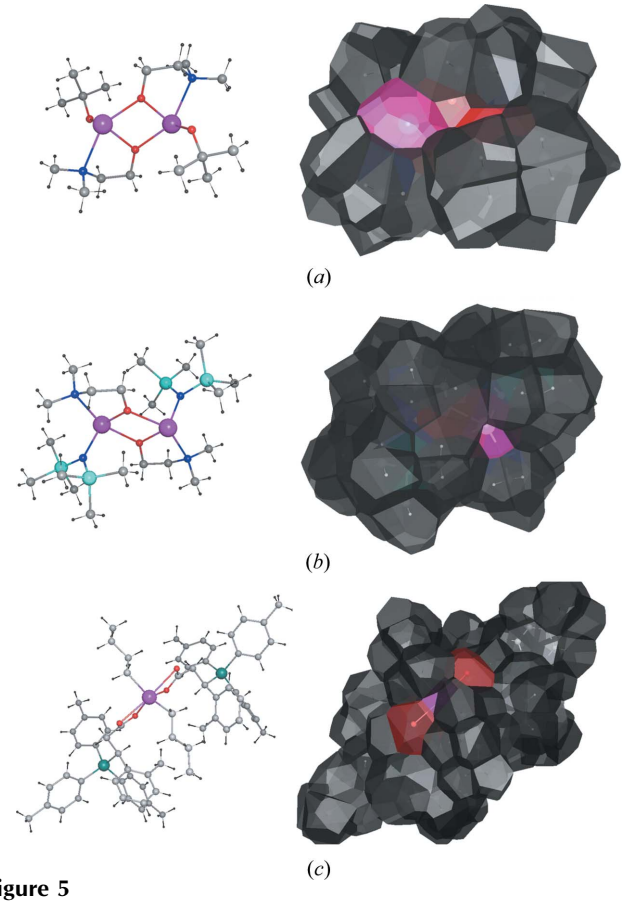

Figure 5
Molecular structure (left) and molecular Voronoi–Dirichlet polyhedra (right) of (*a*) $[Sn^{II}L(^t\mathrm{BuO})]_2$ (Chernov *et al.*, 2009), (*b*) $[Sn^{II}L(N(SiMe_3)_2)]_2$ (Khrustalev, Portnyagin, Zemlyansky, Borisova, Nechaev*et al.*, 2005) and (*c*) $[Sn^{IV}(^n\mathrm{Bu})_2((C_{30}H_{31}Ge)COO)_2]$ (Imtiaz-ud-Din *et al.*, 2003). The faces of Sn, O and H atoms with Rank = 0 are depicted with fuchsia, red and black.

The authors gratefully acknowledge support of Russian Foundation for Basic Research (project 09-03-00669) and of the Foundation of the President of the Russian Federation (project MD-237.2010.3).

References

Abrahams, I., Demetriou, D., Vordemvenne, E., Mustarde, K. & Benoit, D. (2006). *Polyhedron*, **25**, 996–1002.
Abramov, Yu. A. (1997). *Acta Cryst.* A**53**, 264–272.
Allen, F. H. (2002). *Acta Cryst.* B**58**, 380–388.
Armiento, R. & Mattsson, A. E. (2005). *Phys. Rev. B*, **72**, 085108.
Aysin, R. R., Koroteev, P. S., Korlyukov, A. A., Zabula, A. V., Bukalov, S. S., Leites, L. A., Egorov, M. P. & Nefedov, O. M. (2010). *Russ. Chem. Bull.* **59**, 348–360.
Bader, R. F. W. (1990). *Atoms in Molecules. A Quantum Theory.* Oxford: Clarendon Press.
Barrau, J. & Rima, G. (1998). *Coord. Chem. Rev.* **178–180**, 593–622.
Baul, T. S. B., Masharing, C., Basu, S., Pettinari, C., Rivarola, E., Chantrapromma, S. & Fun, H. (2008). *Appl. Organomet. Chem.* **22**, 114–121.
Baul, T. S. B., Rynjah, W., Willem, R., Biesemans, M., Verbruggen, I., Holeapek, M., de Vos, D. & Linden, A. (2004). *J. Organomet. Chem.* **689**, 4691–4701.
Blatov, V. A. (2004). *Cryst. Rev.* **10**, 249–318.
Blatov, V. A. (2006). *IUCr CompComm Newsl.* **7**, 4–38.
Blatov, V. A. & Serezhkin, V. N. (2000). *Russ. J. Inorg. Chem.* **45**, s105–s222.
Borissova, A. O., Korlyukov, A. A., Antipin, M. Y. & Lyssenko, K. A. (2008). *J. Phys. Chem. A*, **112**, 11519–11522.
Bruker (2005). *APEX*2. Bruker AXS Inc., Madison, Wisconsin, USA.
Chernov, O. V., Smirnov, A. Y., Portnyagin, I. A., Khrustalev, V. N. & Nechaev, M. S. (2009). *J. Organomet. Chem.* **694**, 3184–3189.
Davies, A. G. (2004). *Organotin Chemistry.* Weinheim: Wiley-VCH Verlag GmbH and Co.
Dove, A. P., Gibson, V. C., Marshall, E. L., Rzepa, H. S., White, A. J. & Williams, D. J. (2006). *J. Am. Chem. Soc.* **128**, 9834–9843.
Egorov, M. & Gaspar, P. (1995). *Encyclopedia of Inorganic Chemistry.* New York: Wiley.
Espinosa, E., Molins, E. & Lecomte, C. (1998). *Chem. Phys. Lett.* **285**, 170–173.
Frisch, M. J. *et al.* (2004). *GAUSSIAN*03, Revision C.01. Wallingford, CT: Gaussian Inc.
Gonze, X. *et al.* (2002). *Comput. Mater. Sci.* **25**, 478–492.
Hansen, N. K. & Coppens, P. (1978). *Acta Cryst.* A**34**, 909–921.
Harston, P., Howie, R. A., Wardell, J. L., Doidge-Harrison, S. M. S. V. & Cox, P. J. (1992). *Acta Cryst.* C**48**, 279–281.
Hollingsworth, N., Horley, G. A., Mazhar, M., Mahon, M. F., Molloy, K. C., Haycock, P. W., Myers, C. P. & Critchlow, G. W. (2006). *Appl. Organomet. Chem.* **20**, 687–695.
Hori, Y. & Hagiwara, T. (1999). *Int. J. Biol. Macromol.* **25**, 237–245.

Imtiaz-ud-Din, Mazhar, M., Dastgir, S., Mahon, M. F. & Molloy, K. C. (2003). *Appl. Organomet. Chem.* **17**, 801–802.
Keith, T. A. (2009). *AIMALL*, Version 09.04.23, http://aim.tkgristmill.com/.
Khrustalev, V. N., Chernov, O. V., Aysin, R. R., Portnyagin, I. A., Nechaev, M. S. & Bukalov, S. S. (2008). *Dalton Trans.* pp. 1140–1143.
Khrustalev, V. N., Portnyagin, I. A., Nechaev, M. S., Bukalov, S. S. & Leites, L. A. (2007). *Dalton Trans.* pp. 3489–3492.
Khrustalev, V. N., Portnyagin, I. A., Zemlyansky, N. N., Borisova, I. V., Nechaev, M. S., Ustynyuk, Y. A., Antipin, M. Y. & Lunin, V. (2005). *J. Organomet. Chem.* **690**, 1172–1177.
Khrustalev, V. N., Portnyagin, I. A., Zemlyansky, N. N., Borisova, I. V., Ustynyuk, Y. A. & Antipin, M. Y. (2005). *J. Organomet. Chem.* **690**, 1056–1062.
Khrustalev, V. N., Zemlyansky, N. N., Borisova, I. V., Kuznetsova, M. G., Krut'ko, E. B. & Antipin, M. Y. (2007). *Russ. Chem. Bull.* **56**, 267–270.
Kirzhnitz, D. A. (1957). *Sov. Phys. JETP*, **6**, 64–72.
Koritsansky, T. S., Howard, S. T., Richter, T., Macchi, P., Volkov, A., Gatti, C., Mallinson, P. R., Su, S. & Hansen, N. K. (2003). *XD*. Freie University, Berlin, Germany.
Kresse, G. & Furthmuller, J. (1996*a*). *Comput. Mater. Sci.* **6**, 15–50.
Kresse, G. & Furthmuller, J. (1996*b*). *Phys. Rev. B*, **54**, 11169.
Kresse, G. & Hafner, J. (1993). *Phys. Rev. B*, **47**, 558.
Kumar, M. S., Upreti, S., Gupta, H. P. & Elias, A. J. (2006). *J. Organomet. Chem.* **691**, 4708–4716.
Lewis, R. J. (2000). *Sax's Dangerous Properties of Industrial Materials.* New York: Wiley.
Lo, K. M., Kumar Das, V. G. & Ng, S. W. (1999). *Acta Cryst.* C**55**, 1234–1236.
Lu, J., Chen, S., Du, M. & Tang, L. (2006). *Appl. Organomet. Chem.* **20**, 448–453.
Luo, Y.-R. (2007). *Comprehensive Handbook of Chemical Bond Energies.* Boca Raton: CRC Press.
Malcolm, N. O. J., Gillespie, R. J. & Popelier, P. L. A. (2002). *J. Chem. Soc. Dalton Trans.* pp. 3333–3341.
Mattsson, A. E. & Mattsson, T. R. (2009). *J. Chem. Theory Comput.* **5**, 887–894.
Nechaev, M. S. & Ustynyuk, Y. A. (2005). *Russ. Chem. Bull.* **54**, 108–116.
Neumann, W. P. (1991). *Chem. Rev.* **91**, 311–334.
Orita, A., Sakamoto, K., Hamada, Y., Mitsutome, A. & Otera, J. (1999). *Tetrahedron*, **55**, 2899–2910.
Portnyagin, I. A., Nechaev, M. S., Khrustalev, V. N., Zemlyansky, N. N., Borisova, I. V., Antipin, M. Y., Ustynyuk, Y. A. & Lunin, V. V. (2006). *Eur. J. Inorg. Chem.* pp. 4271–4277.
Royal Society of Chemistry (1999). *DOSE, Dictionary of Substances and Their Effects.* Cambridge: Royal Society of Chemistry.
Sheldrick, G. M. (1998). *SADABS*, Version 2.01. Bruker AXS, Madison, Wisconsin, USA.
Sheldrick, G. M. (2008). *Acta Cryst.* A**64**, 112–122.
Silvi, B. & Savin, A. (1994). *Nature*, **371**, 683–686.
Stash, A. & Tsirelson, V. (2002). *J. Appl. Cryst.* **35**, 371–373.
Stoltzfus, M. W., Woodward, P. M., Seshadri, R., Klepeis, J. H. & Bursten, B. (2007). *Inorg. Chem.* **46**, 3839–3850.
Strenalyuk, T., Samdal, S. & Volden, H. V. (2008). *J. Phys. Chem. A*, **112**, 10046–10052.
Su, Z. & Coppens, P. (1998). *Acta Cryst.* A**54**, 646–652.
Tikhonova, I., Tugashov, K., Dolgushin, F., Korlyukov, A., Petrovskii, P., Klemenkova, Z. & Shur, V. (2009). *J. Organomet. Chem.* **694**, 2604–2610.
Tsirelson, V. & Stash, A. (2002). *Chem. Phys. Lett.* **351**, 142–148.
Vologzhanina, A. V., Korlyukov, A. A. & Antipin, M. Y. (2008). *Acta Cryst.* B**64**, 448–455.
Wakamatsu, K., Orita, A. & Otera, J. (2008). *Organometallics*, **27**, 1092–1097.
Win, Y. F., Teoh, S.-G., Ibrahim, P., Ng, S.-L. & Fun, H.-K. (2007*a*). *Acta Cryst.* E**63**, m667–m669.
Win, Y. F., Teoh, S.-G., Ibrahim, P., Ng, S.-L. & Fun, H.-K. (2007*b*). *Acta Cryst.* E**63**, m875–m877.
Zemlyansky, N. N., Borisova, I. V., Kuznetsova, M. G., Khrustalev, V. N., Ustynyuk, Y. A., Nechaev, M. S., Lunin, V. V., Barrau, J. & Rima, G. (2003). *Organometallics*, **22**, 1675–1681.